Grenze International Journal of Engineering and Technology, July Issue

Direct Power Control for a Multilevel Inverter Fed Induction Motor Drive using Predictive Torque Control

Himabindu.T[1], G.Bhuvaneswari[2] and Bhim Singh[3]
[1] Dept. of EEE, BITS-Pilani Hyderabad Campus, Hyderabad, India
Email: hima.bindu210@gmail.com
[2-3] Dept. of EE, IIT Delhi, Delhi, India
Email: {G.Bhuvaneswari, bsingh}@ee.iitd.ac.in

***Abstract*—A novel direct power control (DPC) scheme, with virtual flux orientation based on the grid voltages, has been implemented for an induction motor drive (IMD) fed by an active front end converter (AFEC). The inverter considered here is a multilevel inverter controlled by predictive torque control (PTC). Estimation of instantaneous active (P) and reactive power (Q) of the AFEC is carried out using virtual flux from the main supply. The optimal switching states are selected from the switching table based on the errors in P and Q and hence the active and reactive power control is directly accomplished by the device switching states of the front-end rectifier. Multilevel inverter at the motor side is controlled using a newly proposed PTC algorithm. The proposed algorithm predicts the behavior of the drive under various load conditions which accordingly sets the power requirement for the AFEC. The optimal voltage vector selection in the proposed algorithm is applied to both rectifier and inverter, which reduces the number of switchings and therefore results in distinguishable reduction in the switching losses. Four quadrant operation of this multi-level inverter fed induction motor drive with DPC at the front end and PTC at the load end is implemented in Matlab/Simulink environment and the results are presented. The performance obtained for the drive with the proposed control configuration under various steady state and transient operating conditions show that the drive possesses an excellent dynamic response apart from having impeccable power quality at the front end.**

***Index Terms*— Direct Power Control (DPC), Predictive Torque Control (PTC), Multilevel Inverter (MLI), Active front end (AFE), Induction Motor Drives (IMD), Total Harmonic Distortion (THD).**

I. INTRODUCTION

Active front end (AFE) rectifiers are being employed in a wide range of applications, such as Distributed Generating systems (DGS), Battery Energy Storage Systems (BESS) and adjustable speed drives (ASDs), to improve the power quality (PQ) at the point of common coupling (PCC). This is because the consumers as well as the utilities are very concerned about maintaining an acceptable level of PQ adhering to the international power quality standards. The quality of power has become a major concern for the consumers as well as utilities due to the proliferation of power converters employed in various applications causing non-

Grenze ID: 01.GIJET.6.2.506

sinusoidal currents to be drawn from the power grid. Various control strategies for these AFE rectifiers, such as, Voltage-Oriented Control (VOC), Direct Power Control (DPC) and predictive control [1], [2], [3] have been proposed in the literature. A systematic approach based on grid virtual flux estimation to develop a new switching lookup table for DPC is proposed in [4] wherein low pass filters are introduced to compensate for the magnitude and phase errors in the proposed method. A new control scheme for an AFE rectifier [5] using modern predictive control (MPC) is proposed in [6]. The proposed control strategy makes use of a two level converter which has 7 possible switching states; so, the cost function of the front end rectifier has predictions for all the seven possible voltage vectors. This application of MPC is restricted to those plants whose input is a finite set. DPC strategy applied to a three level neutral point clamped (NPC) converter is presented in [7]. A generalized scheme for DPC in multi-level inverters (MLIs) is proposed in [8] which is validated on a cascaded H-bridge converter for grid-tied applications. In this paper, individual DC link capacitor voltage of each of the H bridges is controlled by selecting suitable space vectors such that power sharing among different H bridges happen in proportion to their rating. The advent of many fast and powerful microprocessors and digital signal processors have enabled the development of many new control techniques for modern power converters such as model adaptive reference controller (MARC) and predictive controllers [9],[10]. Predicting the future behaviour of a system is the main characteristic of a model predictive control (MPC) algorithm. At lower switching frequencies, if torque and current pulsations have to be reduced in an induction motor drive (IMD), it is essential to use advanced control techniques like forced machine current control (FMCC) and model predictive direct current control (MPDCC). A comparison between FMCC and MPDCC is carried out in [11]. In [12], a combination of a PI controller and predictive dead-beat controller is employed in order to achieve fast torque and flux responses, when sufficient voltage reserve is available. There have been research papers on the predictive direct power control (P-DPC) schemes for DC/AC converters [13] and medium voltage grid connected three level neutral point clamped converters [14]. These control strategies have frequently been used for integration of renewable energy sources to the grid and also for motor drives. Predictive optimal switching sequence direct power control of a two level converter is presented in [15], which is computationally intensive although the output response is excellent. Direct torque and predictive torque control methods for a three level reduced switch inverter fed IMD are presented in [16]. A simplified torque control strategy with efficient zero vector placement effecting switching loss reduction in two level VSI fed IMD is proposed in [17]. The present work combines the optimal zero vector placement strategy for switching loss reduction for the multi-level inverter with direct power control of the active front end rectifier. Direct power control of three phase active rectifier proposed with optimal voltage vector selection is carried out based on the estimation of grid virtual flux. This enables the control strategy to calculate instantaneous active and reactive powers. On the load side, three level neutral point clamped inverter fed IMD is controlled using the proposed PTC algorithm with optimal zero vector placement that reduces the switching losses. This analysis is carried out in MATLAB/Simulink environment for dynamic operating conditions in all four quadrants of drive operation. The paper is organized as follows: After an introduction to the problem at hand in Section I, the proposed direct predictive power control algorithm is explained in Section II. Section III presents the modelling aspects of the proposed drive scheme followed by simulation results in Section IV. Section V gives the conclusion drawn out of this work.

II. Modelling of the Proposed DPC for a Back-To-Back Connected Multilevel Converter Fed IMD

A. Direct Power Control

A block diagram of the proposed technique is represented in Fig. 1. First the three-phase balanced voltages and line currents are converted into two-phase form by making use of Clarke's transformation [18].

$$\begin{bmatrix} \hat{v}_a \\ \hat{v}_b \\ \hat{v}_c \end{bmatrix} = \sqrt{\frac{2}{3}} \begin{bmatrix} 1 & 0 \\ \frac{-1}{2} & \frac{\sqrt{3}}{2} \\ \frac{-1}{2} & \frac{-\sqrt{3}}{2} \end{bmatrix} \begin{bmatrix} \hat{v}_\alpha \\ \hat{v}_\beta \end{bmatrix} \tag{1}$$

$$\begin{bmatrix} i_\alpha \\ i_\beta \end{bmatrix} = \sqrt{\frac{2}{3}} \begin{bmatrix} 1 & \frac{-1}{2} & \frac{-1}{2} \\ 0 & \frac{\sqrt{3}}{2} & \frac{-\sqrt{3}}{2} \end{bmatrix} \begin{bmatrix} i_a \\ i_b \\ i_c \end{bmatrix} \tag{2}$$

where v_a, v_b, v_c are three phase power source voltages and i_a, i_b, i_c are three phase line currents. The instantaneous real power and reactive power can be calculated from these transformed voltages and currents as [19] :

$$p = v_\alpha i_\alpha + v_\beta i_\beta \qquad (3)$$

and

$$q = v_\alpha i_\beta - v_\beta i_\alpha \qquad (4)$$

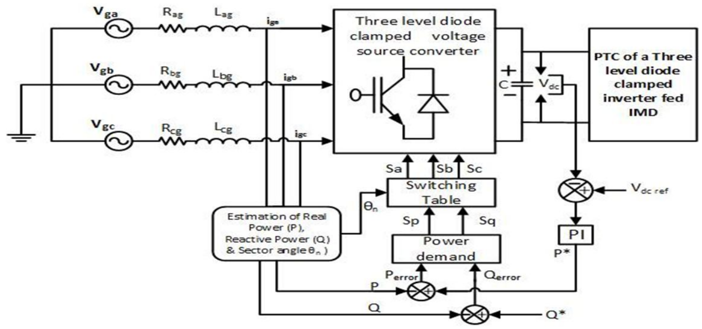

Figure 1. Block diagram of Modelling of the proposed DPC for a back-to-back connected Multilevel converter fed IMD

The real power and reactive power thus calculated could be compared with the reference values of real power and reactive power obtained from the error in the DC link capacitor voltage and the set value of Q respectively, in a hysteresis comparator [20] whose rules are given below:

$$S_p = \begin{cases} 1 & \Delta p \in (h_p, +\infty) \\ 0 & \Delta p \in (-\infty, -h_p) \end{cases} \qquad (5)$$

$$S_q = \begin{cases} 1 & \Delta q \in (h_q, +\infty) \\ 0 & \Delta q \in (-\infty, -h_q) \end{cases} \qquad (6)$$

The virtual flux vector position of the source voltages is calculated as follows: Neglecting resistances of all the components involved, flux vector along *alpha* axis and *beta* axis are given by:

$$\psi_\alpha = \int v_\alpha \, dt \qquad (7)$$

$$\psi_\beta = \int v_\beta \, dt \qquad (8)$$

Angular position of the flux space vector is given by:

$$\theta = \tan^{-1}\left(\frac{\psi_\beta}{\psi_\alpha}\right) \qquad (9)$$

For the errors in p and q, and the virtual flux vector position of the source voltages, the switching table for the three-level neutral point clamped inverter is given in Table 1 as per the sector positions specified in Fig. 2. If θ calculated from equation (9) is lying within a particular range then, it is supposed to be specified as Sector1, Sector 2 and so on as given by equation (10).

$$(n-2)\frac{\pi}{6} \le \theta_n < (n-1)\frac{\pi}{6} \qquad (10)$$

∵ n = 1,2,…,12.

TABLE I. SWITCHING TABLE FOR DIRECT INSTANTANEOUS POWER CONTROL

Sp	Sq	θ_1	θ_2	θ_3	θ_4	θ_5	θ_6	θ_7	θ_8	θ_9	θ_{10}	θ_{11}	θ_{12}
0	0	V_1	V_2	V_3	V_4	V_5	V_6	V_7	V_8	V_9	V_{10}	V_{11}	V_{12}
0	1	V_2	V_3	V_4	V_5	V_6	V_7	V_8	V_9	V_{10}	V_{11}	V_{12}	V_1
1	0	V_{13}	V_{21}	V_{14}	V_{22}	V_{15}	V_{23}	V_{16}	V_{24}	V_{17}	V_{25}	V_{18}	V_{26}
1	1	V_{14}	V_{22}	V_{15}	V_{23}	V_{16}	V_{24}	V_{17}	V_{25}	V_{18}	V_{26}	V_{13}	V_{21}

Table 1 yields the switching positions of various devices in the AFE rectifier which would make sure that reference p and q values are adhered to within an error margin tolerated by the hysteresis controller.

B. Predictive Torque Control of the IMD

The objective of the PTC method is to control the behavior of the system by comparing the future (predicted) values of the IMD system i.e, torque and stator flux with the existing torque and stator flux values [21]. The three main stages involved in this control algorithm, as shown in Fig. 3 are: (i) estimation of variables, (ii)

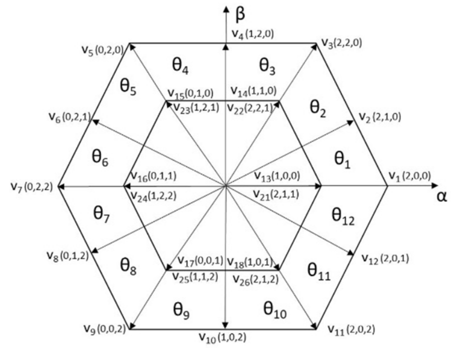

Figure 2. Twelve sectors on Stationary Reference Frame to specify flux vector position

prediction of the future values of the controlled variables, (iii) error minimization by applying the most suitable forcing function which results in minimum error of the controlled variable. In the first stage, a and b phase stator currents (i_a , i_b) are sensed in order to calculate the present values of space phasor variables such as stator flux (ψ_s), rotor flux (ψ_r) and stator current (i(s)).

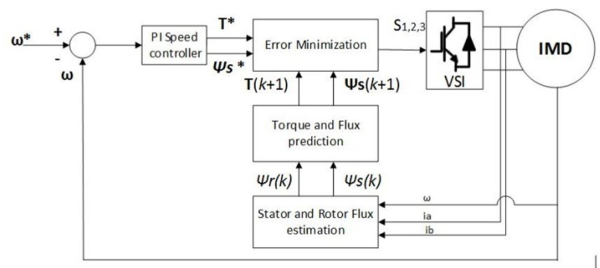

Figure 3. Block diagram of PTC method

The estimated values of stator and rotor flux at k^{th} instant for a sampling time of T_s are given by following equations:

$$\hat{\psi}_s(k) = \hat{\psi}_s(k-1) + T_s V_h(k) - R_s T_s i_s(k) \quad (11)$$

$$\hat{\psi}_r(k) = \frac{L_r}{L_m}\hat{\psi}_s(k) + i_s(k)\left(L_m - \frac{L_r L_s}{L_m}\right) \quad (12)$$

where L_m, L_r, L_s, R_s are machine parameters and V_h is the inverter voltage. The future values, i.e. at $(k+1)^{th}$ instant, of controlled variables are computed during second stage. The prediction of stator flux $\psi_s^p(k+1)$ is given as:

$$\psi_s^p\,(k+1) = \hat{\psi}_s(k) + T_s V_h(k) - R_s T_s i_s(k) \quad (13)$$

$$T^p(k+1) = \frac{3P}{2}\, Im\left\{\bar{\psi}_s^p\,(k+1)\; i_s^p\,(k+1)\right\} \quad (14)$$

where P is the number of poles. The torque prediction $T^p(k+1)$ (in Eq.14) depends on the predicted values of stator flux and stator current, where predicted stator current ($i_s^P\ (k+1)$) is:

$$i_s^p\,(k+1) = \left(1 + \frac{T_s}{\tau_\sigma}\right) i_s(k) + \frac{T_s}{\tau_\sigma + T_s}\left[\frac{1}{R_\sigma}\left\{\left(\frac{k_r}{\tau_r} - k_r\, j\omega\right)\hat{\psi}_r\,(k) + V_h(k)\right\}\right] \quad (15)$$

where $k_r = \frac{L_m}{L_r}$, $R_\sigma = R_s + R_r k_r^2$, $\tau_\sigma = \left(1 - \frac{L_m^2}{L_s L_r}\right)\frac{L_s}{R_\sigma}$ and $\tau_r = \frac{L_r}{R_r}$.

The three level NPC inverter (Fig. 4) has 12 active vectors, 6 redundant vectors and zero vector switch combinations (000,111 and 222) (Fig. 2}). For every possible inverter voltage of $V_h(k)$, the predictive controlled variables (stator flux, torque and stator current) are obtained at $(k+1)^{th}$ instant. During final stage, the error minimization is carried out between the reference and predicted values which are given by:

$$\epsilon_h = |T^* - T^p(k+1)_h| + \lambda_\psi\left|\psi_s^* - \psi_s^p(k+1)_h\right| \quad (16)$$

where h ∈ [0, 1,...,18] and λ_ψ is weighting factor. The ratio of nominal torque to nominal flux is defined as weighting factor. The error minimization is carried out and evaluated for every prediction and the voltage vector for which ϵ_h is minimum is selected as the desired switching combination and applied to the inverter.

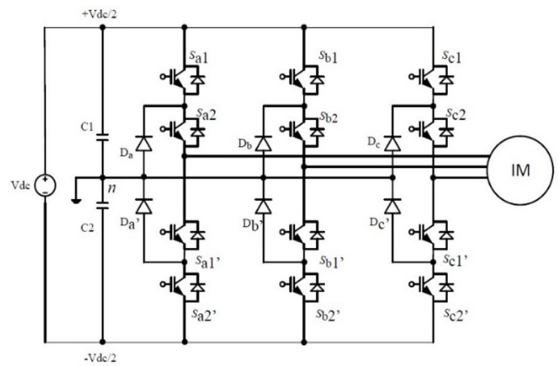

Figure 4. Three level Neutral point clamped VSI fed IMD

III. Modelling of the Proposed Control Algorithm

In a three-level inverter, the redundancy level for zero vector is 3 and for the $V_{dc}/2$ level, the redundancy is 2 as could be seen from the space vector diagram (Fig. 2). The proposed PTC algorithm selects the vector which has the least number of switching transitions from the previous vector whenever any new vector with redundancy is to be applied as shown in Table 2. For example, in one of the time instants, if the voltage vector to be applied is a zero voltage vector (one of V_0, V_{19} or V_{20}), but the previous vector is one of (V_3, V_7, V_{11} or, V_{20}), then according to the proposed logic V_{20} will be applied since this will require only one switch to be transitioned from the previous state to 2 state. On the other hand, if the previous vector had been any one of (V_{14}, V_{16} or V_{18}), then V_{19} would be the choice for the zero vector. Similarly in case of other redundant vector pairs (i.e., V_{13} - V_{21}, V_{14} - V_{22}, V_{15} - V_{23}, V_{16} - V_{24}, V_{17} - V_{25}, V_{18} - V_{26}), if vector V_{23} has to be applied, but the previous vector is one of (V_0, V_2, V_5, V_8, V_{14}, V_{15}, V_{16}), then V_{15} would be applied according to the proposed logic. To put it in a nut shell, the proposed algorithm chooses the voltage vector having the least number of switching transitions from the 'previous' state to the 'next' state whenever there are redundant states available in the 'next' vector.

TABLE II. Proposed $(K+1)^{TH}$ Optimal Voltage Vector Selection Logic

$(k+1)^{th}$ vector to be applied	Previous Voltage Vector
V_0	V_0,V_1, V_5, V_9, V_{13}, V_{15}, V_{17}
V_{20}	V_3, V_7, V_{11}, V_{20}
V_{19}	V_{14}, V_{16}, V_{18}, V_{19}
V_{13}	V_0, V_1, V_4, V_{10}, V_{13}, V_{14}, V_{18}
V_{21}	V_2, V_{12}, V_{16}, V_{19}, V_{21}, V_{22}, V_{26}
V_{14}	V_2, V_4, V_{13}, V_{14}, V_{15}, V_{19}, V_{25}
V_{22}	V_3, V_6, V_{12}, V_{20}, V_{21}, V_{22}, V_{23}
V_{15}	V_0, V_2, V_5, V_8, V_{14}, V_{15}, V_{16}
V_{23}	V_4, V_6, V_{18}, V_{19}, V_{22}, V_{23}, V_{24}
V_{16}	V_6, V_8, V_{15}, V_{16}, V_{17}, V_{19}, V_{21}
V_{24}	V_4, V_7, V_{10}, V_{20}, V_{23}, V_{24}, V_{25}
V_{17}	V_0, V_6, V_9, V_{12}, V_{16}, V_{17}, V_{18}
V_{25}	V_8, V_{10}, V_{14}, V_{19}, V_{24}, V_{25},V_{26}
V_{18}	V_{10}, V_{12}, V_{13}, V_{17}, V_{18}, V_{19}, V_{23}
V_{26}	V_2, V_8, V_{11}, V_{20}, V_{21}, V_{25}, V_{26}

IV. Simulation Results

The proposed algorithm is applied to both three level neutral point clamped rectifier (on the grid side) and multi-level inverter feeding the IMD. The parameters of the IMD are: 3.7 kW, 415 V, 7.5 A, 1425 rpm with pole pairs = 2, L_s = 1.56 H/ph, L_r = 1.56 H/ph, L_m = 1.54 H/ph, R_s = 4.92 Ω/ph, R_r = 6.54 Ω /ph, Machine Inertia (*J*) = 0.0106 *kg-m*^{2}. The inverter switching frequency is 20 kHz.

The performance of the drive with the proposed algorithm is analyzed for all the four quadrants in terms of torque ripples and stator current ripples at load side. Further, the settling time, overshoot and undershoot are observed during different transient and steady state conditions both at grid side and load side as shown in Fig. 5. Both actual and reference values of real power, reactive power (maintained at -500 VAR) are plotted in Fig. 5(a), 5(b) and dc voltage of 600 V is maintained. The steady state peak overshoot of the active power is observed 2310 W and settling time is 0.23 s.

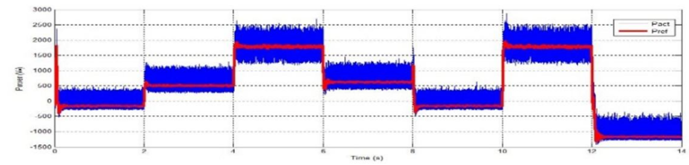

5(a)

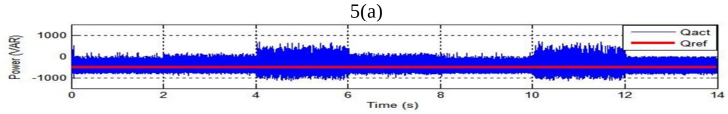

5(b)

Figure 5. Response of (a) Active power (b) Reactive power at different steady and transient state conditions

Fig. 6 shows the performance at load side i.e, three level NPC inverter fed IMD using PTC. Speed at different load conditions is shown in Fig. 6(a) and the Flux is maintained at 1.53 Wb. The load torque (Fig. 6(b)) and a-phase stator current (Fig. 6(c)) ripples at 2 s is observed to be 3% and 4.7%.

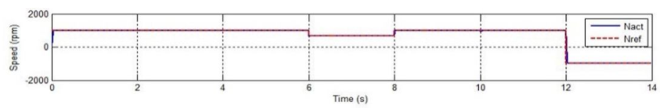

6(a)

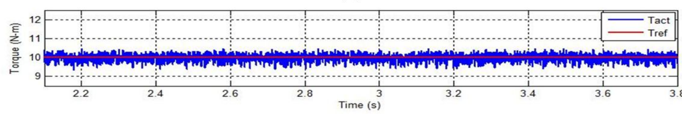

6(b)

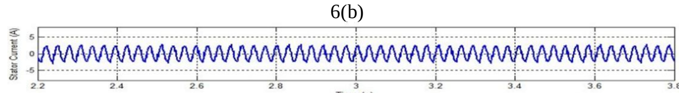

6(c)

Figure 6. Response of the IMD during reference speed change and reversal: (a) Speed (rpm) (b) Torque (N-m) (c) Stator Current (A)

A. Load change with speed constant

The performance of the system for a step change in the load i.e, from 10 N-m to 24 N-m is illustrated in Fig. 7. In this case, the active power at grid side overshoots (Fig. 7(a)) to 2226 W and it settles within 0.06 s, from the time the torque disturbance is created. The peak overshoot in load torque is 20.79% and settling time is about 0.06 s as shown in Fig. 7(b) while the speed is maintained constant at 1000 rpm. However, speed dips to 969 rpm for a short-while during increase in load which bounces back within 3 cycles.

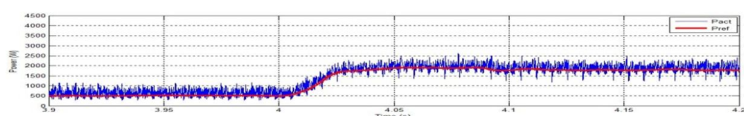

7(a)

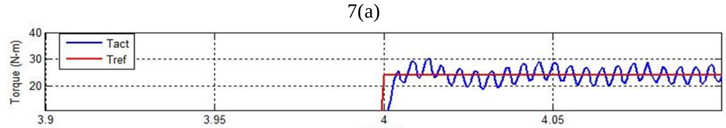

7(b)

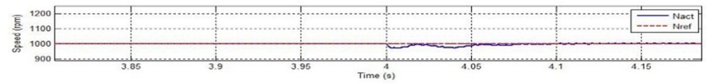

7(c)

Figure 7. Response of (a) Power (W) (b) Torque (N-m) (c) Speed (rpm) when Torque changes from 10 N-m to 24 N-m with speed (1000 rpm) constant

B. Speed change with load constant

The transient behaviour for a sudden change in the reference speed i.e., from 1000 rpm to 680 rpm at 6s while maintaining constant load torque (24 N-m) and repercussion on the grid side are illustrated in Fig. 8. Active power at grid side in Fig. 8(a) dips to 280 W and settles within 0.22 s. At the same time, in order to achieve the fast response of the drive, the torque dips to -36.7 N-m in Fig. 8(b). Fig. 8(c) shows the undershoot in speed that corresponds to 626.7 rpm. However, the speed settles to the reference value within three cycles.

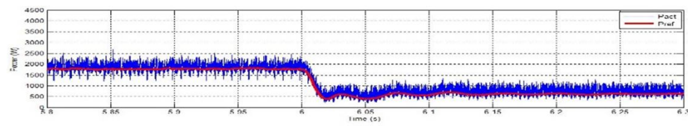

8(a)

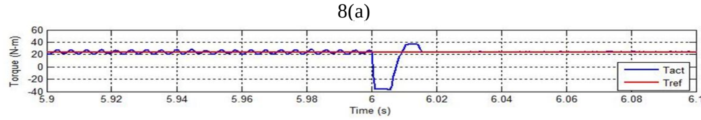

8(b)

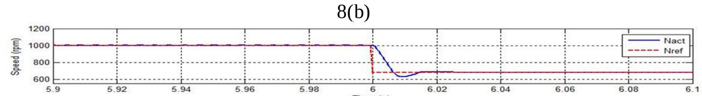

8(c)

Figure 8. Response of (a)Power (W) (b)Torque (N-m) (c) Speed (rpm) when speed changes from 1000 rpm to 680 rpm with load torque constant

Fig. 9 shows the power and speed responses of the drive when speed reversal takes place. The drive takes about 0.06 s for reversal. During this time, the grid side power dips to -1347 W and settles within 0.25 s. The proposed optimal voltage vector selection algorithm is implemented both on three level neutral point clamped rectifier (grid side) and inverter (load side). During the redundant and zero states operation, the efficient voltage vector logic is applied to these converters. Table 3 shows the number of switchings with and without optimal choice of voltage vector at $(k+1)^{th}$ time. The THD analysis in Fig. 9(c) is carried out for the stator current of the IMD, is found to be 2.59% for the switching frequency 20 kHz.

TABLE III. NUMBER OF SWITCHINGS DURING OPTIMAL VOLTAGE VECTOR LOGIC ALGORITHM APPLIED TO BOTH THREE LEVEL NEUTRAL POINT CLAMPED RECTIFIER (GRID SIDE) AND INVERTER (LOAD SIDE) AT $(K+1)^{TH}$ INSTANT

Type of converter	No. of switchings without optimal voltage vector logic at $(k+1)^{th}$ instant (in million)	No. of switchings with optimal voltage vector logic at $(k+1)^{th}$ instant (in million)
Three level rectifier (for DPC)	3.666	0.3647 (90.05% less switching)
Three level inverter (for PTC)	0.5528	0.5282 (4.45% less switching)

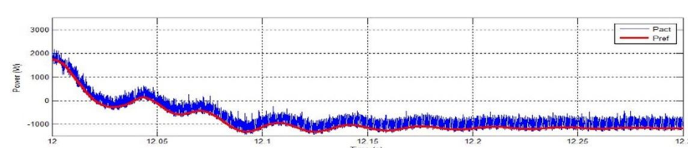

9(a)

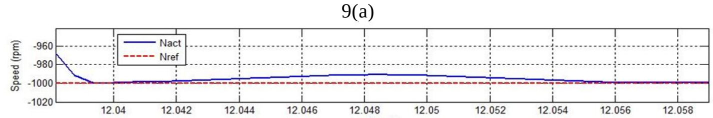

9(b)

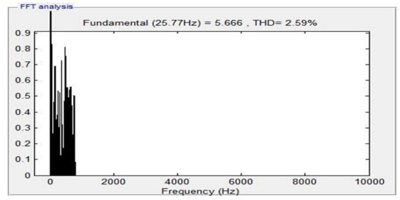

9(c)

Figure 9. Response of IMD during machine reversal (a) Power (W) (b) Speed (rpm) (c) THD analysis for an three level inverter fed IMD using PTC

V. CONCLUSION

The proposed novel control strategies for direct power control on the front end and predictive torque control on the load end is implemented for a multi-level inverter fed IMD. Three level NPC converters are used at the front end as well as load end. The simulated results shows the performance of the active and reactive power of the AFEC. Similarly, torque, speed and stator current variations under different load conditions have been observed for the multi-level inverter fed IMD which is controlled by PTC on the load side. During the switching condition, the choice of selection of optimal voltage vector is done in an optimal manner wherever redundancy exists. Because of this, 90.04% and 4.75% reduction in switchings of the AFE rectifier and multi-level inverter at the motor end, respectively were attained. The THD of the output current at the load side is observed to be 2.59% which is less when compared to classic methods in the literature. The complete behaviour of the system in all the four quadrants not only yields better performance of the drive, but also improves the efficiency since the number of switchings are reduced due to optimal voltage vector logic.

REFERENCES

[1] Yongchang Zhang, Haitao Yang, and Bo Xia, “Model predictive torque control of induction motor drives with reduced torque ripple,” *IET Electric Power Applications*, 9(9):595-604, 2015.

[2] Changliang Xia, Xudong Qiu, Zhiqiang Wang, and Tingna Shi, “Predictive torque control for voltage source inverter-permanent magnet synchronous motor based on equal torque effect,” *IET Electric Power Applications*, 10(3):208-216, 2016.

[3] Igim Kim, Roh Chan, and Sangshin Kwak, “Model predictive control method for chb multi-level inverter with reduced calculation complexity and fast dynamics,” *IET Electric Power Applications*, 11(5):784-792, 2017.

[4] Azziddin M Razali, MA Rahman, Glyn George, and Nasrudin A Rahim, “Analysis and design of new switching lookup table for virtual flux direct power control of grid-connected three-phase pwm ac-dc converter,” *IEEE Transactions on Industry Applications*, 51(2):1189-1200, 2015.

[5] Mohammad Hosein Saeedinia and S Alireza Davari, “Virtual flux model predictive direct power control (vf-mpdpc) of afe rectifier with new current prediction method and negative sequence elimination,” In *Predictive Control of Electrical Drives and Power Electronics (PRECEDE), 2017 IEEE International Symposium on*, pages 113-118. IEEE, 2017.

[6] Patricio Cortes, Jose Rodriguez, Patrycjusz Antoniewicz, and Marian Kazmierkowski, “Direct power control of an afe using predictive control,” *IEEE Transactions on Power Electronics*, 23(5):2516-2523, 2008.

[7] Ning Li, Yue Wang, Su Li, Yufei Li, et al., “Direct power control strategy used in three-level npc converters,” In *Power Electronics and Motion Control Conference (IPEMC), 2012 7th International*, volume 3, pages 1675-1679. IEEE, 2012.

[8] Sebastian Rivera, Samir Kouro, Bin Wu, Salvador Alepuz, Mariusz Malinowski, Patricio Cortes, and Jose Rodriguez, “Multilevel direct power control-a generalized approach for grid-tied multilevel converter applications,” *IEEE Transactions on Power Electronics*, 29(10):5592-5604, 2014.

[9] Saverio Bolognani, Silverio Bolognani, Luca Peretti, and Mauro Zigliotto, “Design and implementation of model predictive control for electrical motor drives,” *IEEE Transactions on industrial electronics*, 56(6):1925-1936, 2009.

[10] Patricio Cortes, Marian P Kazmierkowski, Ralph Kennel, Daniel E Quevedo, and Jose R Rodriguez, “Predictive control in power electronics and drives,” *IEEE Trans. Industrial Electronics*, 55(12):4312-4324, 2008.

[11] James Scoltock, Tobias Geyer, and Udaya Madawala, “A comparison of predictive current control schemes for mv induction motor drives,” *In IECON 2011-37th Annual Conference on IEEE Industrial Electronics Society*, pages 1680 1685. IEEE, 2011.

[12] Pablo Correa, Mario Pacas, and Jos Rodriguez, “Predictive torque control for inverter-fed induction Machines,” *IEEE Transactions on Industrial Electronics*, 54(2):1073-1079, 2007.

[13] Sergio Aurtenechea, Miguel Angel Rodriguez, Estanis Oyarbide, and Jose Ramon Torrealday, "Predictive direct power control-a new control strategy for dc/ac converters," *In IEEE Industrial Electronics, IECON 2006-32nd Annual Conference on*, pages 1661-1666. IEEE, 2006.

[14] S Aurtenechea, MA Rodriguez, Estanis Oyarbide, and JR Torrealday, "Predictive direct power control of mv grid-connected three-level npc converters," In *Industrial Electronics, 2007. ISIE 2007. IEEE International Symposium on*, pages 901-906. IEEE, 2007.

[15] Sergio Vazquez, Abraham Marquez, Ricardo Aguilera, Daniel Quevedo, Jose I Leon, and Leopoldo G Franquelo, "Predictive optimal switching sequence direct power control for grid- connected power converters," *IEEE Transactions on Industrial Electronics*, 62(4):2010-2020, 2015.

[16] T Himabindu, AV Ravi Teja, G Bhuvaneswari, and Bhim Singh, "Predictive torque control of a three- level reduced switch inverter fed induction motor drive," In *Industrial Electronics (ISIE), 2017 IEEE 26th International Symposium on*, pages 348-353. IEEE, 2017.

[17] T Himabindu, AV Ravi Teja, G Bhuvaneswari, and Bhim Singh, "Simplified predictive torque control of an im drive with effcient zero vector placement," In *Industrial Electronics (ISIE), 2017 IEEE 26th International Symposium on*, pages 362-367. IEEE, 2017.

[18] Toshihiko Noguchi, Hiroaki Tomiki, Seiji Kondo, and Isao Takahashi, "Direct power control of pwm converter without power-source voltage sensors," *IEEE Transactions on Industry Applications*, 34(3):473-479, 1998.

[19] Hirofumi Akagi, Yoshihira Kanazawa, and Akira Nabae, "Instantaneous reactive power compensators comprising switching devices without energy storage components," *IEEE Transactions on industry applications*, (3):625-630, 1984.

[20] Wu Wenjun, Zhong Yanru, and Wang Jianjun, "The comparative study of different methods about mconstructing switching table in dpc for three-level rectifier," In *Power Electronics for Distributed Generation Systems (PEDG), 2010 2nd IEEE International Symposium on*, pages 314-319. IEEE, 2010.

[21] Jose Rodriguez and Patricio Cortes, "Predictive control of power converters and electrical drives," volume 40. John Wiley & Sons, 2012.